

Evidence that FeLoBALs may signify the transition between an ultraluminous infrared galaxy and a quasar

D. Farrah¹

M. Lacy²

R. Priddey³

C. Borys⁴

J. Afonso⁵

ABSTRACT

We present mid/far-infrared photometry of nine FeLoBAL QSOs, taken using the *Spitzer* space telescope. All nine objects are extremely bright in the infrared, with rest-frame 1-1000 μ m luminosities comparable to those of Ultraluminous Infrared Galaxies. Furthermore, a significant fraction of the infrared emission from many, and possibly all of the sample is likely to arise from star formation, with star formation rates of order several hundred solar masses per year. We combine these results with previous work to propose that FeLoBALs mark galaxies and QSOs in which an extremely luminous starburst is approaching its end, and in which a rapidly accreting supermassive black hole is in the last stages of casting off its dust cocoon. FeLoBAL signatures in high redshift QSOs and galaxies may thus be an efficient way of selecting sources at a critical point in their evolution.

Subject headings: galaxies: active – quasars: absorption lines – infrared: galaxies – galaxies: evolution

¹Department of Astronomy, Cornell University, Ithaca, NY 14853, USA

²Spitzer Science Center, California Institute of Technology, Pasadena, CA 91125, USA

³Centre for Astrophysics Research, University of Hertfordshire, College Lane, Hatfield AL10 9AB, UK

⁴Department of Astronomy and Astrophysics, University of Toronto, Toronto, Canada

⁵Centro de Astronomia e Astrofísica, Universidade de Lisboa, Lisbon, Portugal

1. Introduction

First seen in 1967 (Lynds 1967), Broad Absorption Line (BAL) QSOs are those objects that show broad, deep troughs in their UV and optical spectra, arising from resonance line absorption in gas outflowing with velocities of $\gtrsim 0.1c$ (Weymann et al. 1991; Arav et al. 2001; Hall et al. 2002; Reichard et al. 2003). BAL QSOs come in three subtypes depending on which absorption features are seen. High Ionization BAL QSOs (HiBALs) show absorption in Ly α , NV λ 1240, SiIV λ 1394 and CIV λ 1549, and comprise about 85% of the BAL population. Low Ionization BAL QSOs (LoBALs) contain all the absorption features seen in HiBALs, and also show absorption in MgII λ 2799 and other low ionization species, and comprise $\sim 15\%$ of the BAL population. Finally, a rare class of BAL QSO, in addition to showing all the absorption lines seen in LoBALs, also show absorption features arising from metastable excited levels of iron. These are termed FeLoBAL QSOs (Hazard et al. 1987; Becker et al. 1997; Branch et al. 2002; Lacy et al. 2002).

Efforts to explain the origin of BALs in QSOs have been ongoing since their discovery. Broadly, there are two possibilities. The first is that BAL QSOs are normal QSOs viewed along a particular line of sight; in this case the absorption features arise when an accretion disk wind encounters a high column density, ionized gas outside the broad line region (Murray & Chiang 1998; Proga et al. 2000). The gas is driven outwards via resonance line absorption, but the high column density of the gas shields it from higher energy photons that would otherwise completely ionize it. In this case, BAL QSOs are those QSOs viewed along a line of sight that coincides with the outflowing gas (Elvis 2000). The second possibility is that BAL QSOs are youthful objects, still surrounded by gas and dust in which the absorption takes place; in this case the BALs do not arise due to a particular line of sight (Voit et al. 1993; Becker et al. 1997; Williams et al. 1999).

There has been significant debate over the years on the best method to find young QSOs (e.g. Sanders et al. 1988; Kawakatu et al. 2006), so the idea that some BAL QSOs may be such objects is particularly intriguing. Most attention has focused on the LoBALs as candidate young QSOs (Lipari et al. 1994; Canalizo & Stockton 2001), as the differences between the line properties of LoBAL QSOs and those of ordinary QSOs are hard to explain solely in terms of different relative orientations (Sprayberry & Foltz 1992). Nevertheless, the picture of LoBALs being young QSOs is controversial; for example sub-mm observations (Lewis et al. 2003; Willott et al. 2003; Priddey et al. 2007) show no differences between BAL QSOs and ordinary QSOs. Furthermore, Voit et al. (1993) propose a scenario in which LoBALs form via ablation of dust by UV photons in outflows arranged either as a thick disk or as an isotropic distribution of clouds; in this case LoBALs do fit within AGN orientation schemes, and this scenario is consistent with polarimetric observations (Schmidt & Hines

1999; Ogle et al. 1999; Hutsemékers & Lamy 2000).

Recently however, evidence has mounted that FeLoBAL QSOs may be the strongest candidates for being youthful QSOs. Based on UV and optical spectra, Hall et al. (2002) suggest that FeLoBALs are young objects still surrounded by a dust cocoon. Similar conclusions are reached by Gregg et al. (2002), who also postulate that FeLoBALs may be associated with galaxy interactions. Further evidence comes from observations of the only two known FeLoBALs at $z < 0.15$, both of which are associated with Ultraluminous Infrared Galaxies (ULIRGs, e.g. Farrah et al. 2005). Finally, the presence of winds with large spatial extents ($\gtrsim 100\text{pc}$) in some FeLoBAL QSOs (de Kool et al. 2002) provides a plausible mechanism for an emerging QSO to directly affect the star formation. Although selection effects may play a role, this lends weight to the idea that FeLoBALs and ULIRGs are linked in some way.

It is plausible therefore that the Fe absorption seen in FeLoBALs arises from iron injected into the ISM by an ongoing or recent starburst; marking the FeLoBAL phenomenon as a transition stage in a ULIRG when the starburst is at or near its end, and the central QSO is starting to throw off its dust cocoon. In this letter we examine the validity of this speculation, by observing a sample of nine FeLoBAL QSOs using the Multiband Imaging Photometer for Spitzer (Rieke et al. 2004) onboard the *Spitzer* space telescope (Werner et al. 2004). We assume a spatially flat cosmology, with $H_0 = 70 \text{ km s}^{-1} \text{ Mpc}^{-1}$, $\Omega = 1$, and $\Omega_\Lambda = 0.7$. Unless otherwise stated, the term ‘IR luminosity’ refers to the total luminosity integrated over 1-1000 μm in the rest-frame.

2. Observations

Due to their rarity, assembling a homogenous sample of FeLoBAL QSOs is not trivial. At the time of writing this paper a few hundred FeLoBALs are known (Trump et al. 2006), but when the proposal was being written only 40 or so FeLoBAL QSOs were known over the whole sky, most of which lay at $z > 1$. We therefore aimed to select a sample that spanned a relatively narrow redshift range, and gave a reasonable sampling of the properties of FeLoBAL QSOs, at the expense of homogeneity, with the broader goal of obtaining a qualitative idea of the range of their infrared properties. We imposed an upper redshift cut of $z = 1.8$ and a lower redshift cut of $z=1.0$. We then randomly selected nine objects. Six of these objects were found via spectroscopic observations of the Sloan Digital Sky Survey (Hall et al. 2002), one (ISO J0056-2738) was discovered serendipitously from followup of distant clusters that had been surveyed with ISO (Duc et al. 2002), one (FBQS J1427+2709) was discovered during spectroscopic followup of radio loud quasar candidates from the FIRST survey (Becker et al. 1997), and one is the ‘archetype’ FeLoBAL QSO LBQS 0059-2735

(Hazard et al. 1987). The full sample is listed in Table 1.

Seven of the sample were observed in July 2006, one (SDSS J0338+0056) was observed in February 2007, and one (LBQS 0059-2735) was observed in March 2004, using MIPS at $24\mu\text{m}$, $70\mu\text{m}$ and $160\mu\text{m}$ (PIDs 30299 & 82). Following observation, the raw data were processed automatically with the MIPS data reduction pipeline at the Spitzer Science Center, which performs standard tasks such as image coaddition, sky and dark subtraction, and bias removal. We inspected the output frames from this pipeline, and determined that they were of sufficient quality for reasonably accurate ($\sim 10\%$) photometry of our targets, hence no further reduction steps were performed. Photometry was carried out using the ‘digiphot’ package within the Image Reduction Analysis Facility (IRAF) software. We used apertures of 2.45, 2.0 and 2.5 pixels at $24\mu\text{m}$, $70\mu\text{m}$ and $160\mu\text{m}$ to measure the fluxes of our objects, resulting in aperture corrections of 1.698, 3.900 and 3.215 respectively.

3. Results

The MIPS fluxes are presented in Table 1, along with any available archival IR photometry. Four objects are detected in all three MIPS bands, though two of these four are detected only weakly at $160\mu\text{m}$. Three objects are detected at $24\mu\text{m}$ and $70\mu\text{m}$. The remaining two objects are detected only at $24\mu\text{m}$.

In the absence of IR spectroscopy, detailed measurements of the properties of IR-luminous AGN or starbursts in our sample are not possible. We can however constrain both the total IR luminosities, and the contribution from star formation and/or an AGN, by fitting the IR photometry simultaneously with the library of model spectral energy distributions (SEDs) for the emission from a starburst (Efstathiou et al. 2000) and an AGN (Rowan-Robinson 1995), following the methods described in Farrah et al. (2003). These model libraries span a large number of free parameters (e.g. torus opening angle and line of sight for the AGN, burst lifetime and UV opacity for the starbursts) but we here use the complete model libraries solely to estimate the likely range in total, starburst and AGN luminosities that are consistent with the available data. The results are presented in Table 2.

The four objects with detections in all three MIPS bands are all extremely luminous, with IR luminosities exceeding $10^{12.7}L_{\odot}$. In all four objects a starburst is required to explain the $160\mu\text{m}$ emission while remaining consistent with the $24\mu\text{m}$ and $70\mu\text{m}$ points (for LBQS 0059-2735 an AGN model is consistent with the MIPS data, but the detection at $850\mu\text{m}$ requires a starburst component). The predicted starburst luminosities exceed $10^{12.4}L_{\odot}$ in all

cases, with inferred star formation rates of several hundred Solar masses per year. The best fit SEDs for these four objects are given in Figure 1. An example of a pure AGN fit to one of these four objects is shown in Figure 2.

The remaining five objects are not detected at $160\mu\text{m}$, hence the constraints on their luminosities and power sources are cruder. For these five objects we do not present best-fit SEDs, but merely summarize the results. Three of these five objects are detected at $24\mu\text{m}$ and $70\mu\text{m}$, and all have IR luminosities exceeding $10^{12.9}L_{\odot}$. The non-detection at $160\mu\text{m}$ combined with the detection at $70\mu\text{m}$ sets an upper limit on any starburst contribution such that an AGN must supply at least some of the $24\mu\text{m}$ and $70\mu\text{m}$ emission. Indeed, it is possible to explain the $24\mu\text{m}$ and $70\mu\text{m}$ emission in all three objects purely with an AGN model, though a significant starburst contribution is not ruled out. The final two objects are only detected at $24\mu\text{m}$. For one of these (ISO J0056-2738) we also have a $15\mu\text{m}$ flux from ISO (Duc et al. 2002), allowing us to conclude that the bulk of the IR emission likely arises from an AGN. For SDSS J2336-0107 however, we have only a $24\mu\text{m}$ flux, and hence cannot set any meaningful constraints on its IR emission.

4. Discussion

Starting with the results in this paper, we examine the conjecture that FeLoBAL QSOs represent a specific point in an evolutionary sequence between a ULIRG and a ‘classical’ QSO. We initially only consider the total IR luminosities, listed in Table 2. All of our sample are extremely IR-luminous, with luminosities comparable to those of both local ULIRGs (Farrah et al. 2003; Lonsdale et al. 2006) and to high redshift sub-mm bright sources (SMGs, e.g. Blain et al. 2002; Borys et al. 2004). In most cases the upper limits on the IR luminosities exceed $10^{13}L_{\odot}$, making them potentially comparable in luminosity to high redshift Hyperluminous Infrared Galaxies (Rowan-Robinson 2000; Farrah et al. 2002). At time of writing there exists no ‘classical’ QSO sample for which direct comparisons to our sample are valid (i.e. one at $1.0 < z < 1.8$, matched in optical magnitude and observed with MIPS), but it is notable that the IR luminosities of our sample substantially exceed those of nearly all the Palomar-Green QSOs presented by Haas et al. (2003).

We next consider the power source behind the IR emission. In 5/9 objects, the SED fits predict that the IR emission arises at least in part, and possibly entirely, from an AGN, perhaps accompanied by a starburst. In 4/9 objects however, those with detections at longer wavelengths, the SED fits demand that a substantial fraction of the total IR emission arises from star formation, with implied star formation rates of order a few hundred solar masses per year. This implies that FeLoBAL QSOs are preferentially associated with obscured,

luminous starbursts that are comparable to the starbursts that are thought to power the majority of the IR emission from both local ULIRGs and distant SMGs. There is the caveat that our sample is heterogenous, but if we restrict attention to only the six QSOs selected from the SDSS, then the fraction of sources with starbursts, at 2/6, remains equivalent within the errors, though the small sample sizes render these conclusions tentative at best.

A potentially more serious caveat however is that the results in Table 2 are dependent on the assumption that the SED libraries used in the fitting span the range in SED shapes of observed IR-luminous starbursts and AGN. This assumption is a reasonable one, given that these same SED libraries give good fits to the SEDs of local ULIRGs, and predict starburst and AGN luminosities that are consistent with results from other wavelengths (Farrah et al. 2003). There is, however, one scenario we cannot test for. Although we find that a luminous starburst must be present in the four objects detected at $160\mu\text{m}$, there do exist models for the dust distributions around AGN where the dust is so extended (several tens of parsecs) that its outer regions are cold enough to emit significantly at wavelengths longward of $100\mu\text{m}$. Such an extended dust distribution could account for some or all of the $160\mu\text{m}$ emission in these four objects. We cannot formally exclude this scenario, but note that interferometric observations of local AGN have found no evidence supporting such extended dust distributions (e.g. Jaffe et al. (2004)). We therefore do not consider this possibility to be likely.

Finally, we consider our results together with those from previous work. Prior evidence that suggests links between FeLoBAL QSOs and ULIRGs includes; (1) the only two systems at low redshifts known to contain FeLoBALs are both ULIRGs (e.g. Farrah et al. 2005), (2) FeLoBAL QSOs at high redshifts may be involved in interactions (Gregg et al. 2002), and (3) large-scale winds in FeLoBAL QSOs may provide a mechanism for the emerging AGN to affect star formation in the host galaxy (de Kool et al. 2002). To these we add (4) FeLoBAL QSOs are, as a class, extremely IR-luminous, with IR luminosities comparable to those of ULIRGs at low and high redshifts, and (5) star formation powers a significant fraction of the IR emission in many, and possibly all, FeLoBAL QSOs, with implied star formation rates comparable to those inferred for local and high redshift ULIRGs. Overall therefore, our results combine with those from previous work to construe strong, albeit indirect evidence for evolutionary links between FeLoBAL QSOs and ULIRGs. We therefore propose that FeLoBALs mark galaxies and QSOs in which an extremely luminous starburst is approaching its end, and in which a rapidly accreting supermassive black hole is in the last stages of casting off its dust cocoon. FeLoBAL signatures in high redshift QSOs and galaxies may thus be an efficient way of selecting sources at a critical point in their evolution.

We thank the referee for a very helpful report. This work is based on observations

made with the Spitzer Space Telescope, which is operated by the Jet Propulsion Laboratory, California Institute of Technology under a contract with NASA. Support for this work was provided by NASA. This research has made extensive use of the NASA/IPAC Extragalactic Database (NED) which is operated by the Jet Propulsion Laboratory, California Institute of Technology, under contract with NASA. JA acknowledges support from the Science and Technology Foundation (Portugal) through the research grant POCI/CTE-AST/58027/2004. RSP thanks the University of Hertfordshire for support.

REFERENCES

- Arav, N., et al. 2001, *ApJ*, 561, 118
- Becker, R. H., Gregg, M. D., Hook, I. M., McMahon, R. G., White, R. L., & Helfand, D. J. 1997, *ApJ*, 479, L93
- Blain, A. W., Smail, I., Ivison, R. J., Kneib, J.-P., & Frayer, D. T. 2002, *Phys. Rep.*, 369, 111
- Borys, C., Scott, D., Chapman, S., Halpern, M., Nandra, K., & Pope, A. 2004, *MNRAS*, 355, 485
- Branch, D., Leighly, K. M., Thomas, R. C., & Baron, E. 2002, *ApJ*, 578, L37
- Canalizo, G., & Stockton, A. 2001, *ApJ*, 555, 719
- Clavel, J. 1998, *A&A*, 331, 853
- Duc, P.-A., et al. 2002, *A&A*, 389, L47
- Efstathiou, A., Rowan-Robinson, M., & Siebenmorgen, R. 2000, *MNRAS*, 313, 734
- Elvis, M. 2000, *ApJ*, 545, 63
- Farrah, D., Serjeant, S., Efstathiou, A., Rowan-Robinson, M., & Verma, A. 2002, *MNRAS*, 335, 1163
- Farrah, D., Afonso, J., Efstathiou, A., Rowan-Robinson, M., Fox, M., & Clements, D. 2003, *MNRAS*, 343, 585
- Farrah, D., Surace, J. A., Veilleux, S., Sanders, D. B., & Vacca, W. D. 2005, *ApJ*, 626, 70
- Gregg, M. D., Becker, R. H., White, R. L., Richards, G. T., Chaffee, F. H., & Fan, X. 2002, *ApJ*, 573, L85

- Haas, M., et al. 2003, *A&A*, 402, 87
- Hall, P. B., et al. 2002, *ApJS*, 141, 267
- Hazard, C., McMahon, R. G., Webb, J. K., & Morton, D. C. 1987, *ApJ*, 323, 263
- Hutsemékers, D., & Lamy, H. 2000, *A&A*, 358, 835
- Jaffe, W., et al. 2004, *Nature*, 429, 47
- Kawakatu, N., Anabuki, N., Nagao, T., Umemura, M., & Nakagawa, T. 2006, *ApJ*, 637, 104
- de Kool, M., Becker, R. H., Arav, N., Gregg, M. D., & White, R. L. 2002, *ApJ*, 570, 514
- Lacy, M., Gregg, M., Becker, R. H., White, R. L., Glikman, E., Helfand, D., & Winn, J. N. 2002, *AJ*, 123, 2925
- Lewis, G. F., Chapman, S. C., & Kuncic, Z. 2003, *ApJ*, 596, L35
- Lipari, S., Colina, L., & Macchetto, F. 1994, *ApJ*, 427, 174
- Lonsdale, C. J., Farrah, D., & Smith, H. E. 2006, *Astrophysics Update* 2, 285, *astroph* 0603031
- Lynds, C. R. 1967, *ApJ*, 147, 837
- Murray, N., & Chiang, J. 1998, *ApJ*, 494, 125
- Ogle, P. M., Cohen, M. H., Miller, J. S., Tran, H. D., Goodrich, R. W., & Martel, A. R. 1999, *ApJS*, 125, 1
- Priddey, R. S., Gallagher, S. C., Isaak, K. G., Sharp, R. G., McMahon, R. G., & Butner, H. M. 2007, *MNRAS*, 374, 867
- Proga, D., Stone, J. M., & Kallman, T. R. 2000, *ApJ*, 543, 686
- Reichard, T. A., et al. 2003, *AJ*, 126, 2594
- Rieke, G. H., et al. 2004, *ApJS*, 154, 25
- Rowan-Robinson, M. 1995, *MNRAS*, 272, 737
- Rowan-Robinson, M. 2000, *MNRAS*, 316, 885
- Sanders, D. B., Soifer, B. T., Elias, J. H., Madore, B. F., Matthews, K., Neugebauer, G., & Scoville, N. Z. 1988, *ApJ*, 325, 74

Schmidt, G. D., & Hines, D. C. 1999, *ApJ*, 512, 125

Sprayberry, D., & Foltz, C. B. 1992, *ApJ*, 390, 39

Trump, J. R., et al. 2006, *ApJS*, 165, 1

Voit, G. M., Weymann, R. J., & Korista, K. T. 1993, *ApJ*, 413, 95

Werner, M. W., et al. 2004, *ApJS*, 154, 1

Weymann, R. J., Morris, S. L., Foltz, C. B., & Hewett, P. C. 1991, *ApJ*, 373, 23

Williams, R. J. R., Baker, A. C., & Perry, J. J. 1999, *MNRAS*, 310, 913

Willott, C. J., Rawlings, S., & Grimes, J. A. 2003, *ApJ*, 598, 909

Table 1. FeLoBAL QSO Sample, and infrared photometry

Galaxy	RA (J2000)	Dec	z	m_i	f_{15}	f_{24}	f_{70}	f_{160}	f_{450}^a	f_{850}^a
ISO J005645.1-273816	00 56 45.15	-27 38 15.6	1.78	20.95 ^f	1.33 ^b	1.56	<7.0	<50	–	–
LBQS 0059-2735	01 02 17.02	-27 19 48.8	1.59	17.39 ^f	–	7.83	19.9	29.0 ^d	<168.9	10.3
SDSS J033810.85+005617.6	03 38 10.85	+00 56 17.6	1.63	18.33	–	2.02	8.4	55.5 ^e	–	–
SDSS J115436.60+030006.3	11 54 36.60	+03 00 06.4	1.46	17.74	–	7.59	17.9	<50	–	–
SDSS J121441.42-000137.8	12 14 41.43	-00 01 37.9	1.05	18.77	–	4.69	38.3	78.9	–	–
FBQS J142703.6+270940	14 27 03.64	+27 09 40.3	1.17	18.11	–	4.76	32.6	68.1	–	–
SDSS J155633.78+351757.3	15 56 33.80	+35 17 58.0	1.50	18.01	8.30 ^c	13.93	24.7	<50	<86.1	<3.6
SDSS J221511.93-004549.9	22 15 11.94	-00 45 49.9	1.48	16.49	–	10.4	27.2	<50	–	–
SDSS J233646.20-010732.6B	23 36 45.10	-01 07 32.4	1.29	21.73	–	0.48	<7.0	<50	–	–

Note. — All fluxes are quoted in mJy. The ‘small’ field size was used for all three channels, using the default pixel scale at $70\mu\text{m}$. Exposure times per cycle and number of cycles for all sources except LBQS 0059-2735 were 30s, 10s, 10s and 5, 7 and 4 respectively, giving on-source exposure times of 2260s, 755s and 85s. For LBQS 0059-2735 the exposure times were shorter; 3s, 10s and 10s with 1, 1, and 3 cycles respectively. Errors are typically 10% on the $24\mu\text{m}$ fluxes, 20% on the $70\mu\text{m}$ fluxes, and 25% on the $160\mu\text{m}$ fluxes. Limits are 3σ .

^aLewis et al. (2003)

^bDuc et al. (2002)

^cClavel (1998)

^d 2σ detection

^e 2.7σ detection

^fR band magnitude

Table 2. Infrared Luminosities

Galaxy	L_{tot}	L_{AGN}	L_{SB}
ISO J0056-2738	12.48-13.00	12.40-13.00	<12.90
LBQS 0059-2735	12.95-13.20	12.80-13.00	12.44-12.82
SDSS J0338+0056	12.90-13.40	<12.40	12.60-13.40
SDSS J1154+0300	12.89-13.10	12.70-12.95	<12.98
SDSS J1214-0001	12.70-12.88	<12.44	12.68-12.84
FBQS J1427+2709	12.81-13.01	<12.70	12.70-13.00
SDSS J1556+3517	13.10-13.30	12.90-13.23	<12.50
SDSS J2215-0045	13.00-13.40	12.50-13.40	<12.80
SDSS J2336-0107	11.70-12.90	–	–

Note. — Quoted luminosities are the logarithm of the rest-frame 1-1000 μm luminosity, in units of solar luminosities (3.826×10^{26} Watts), derived from the SED fits. Limits and ranges are 3σ .

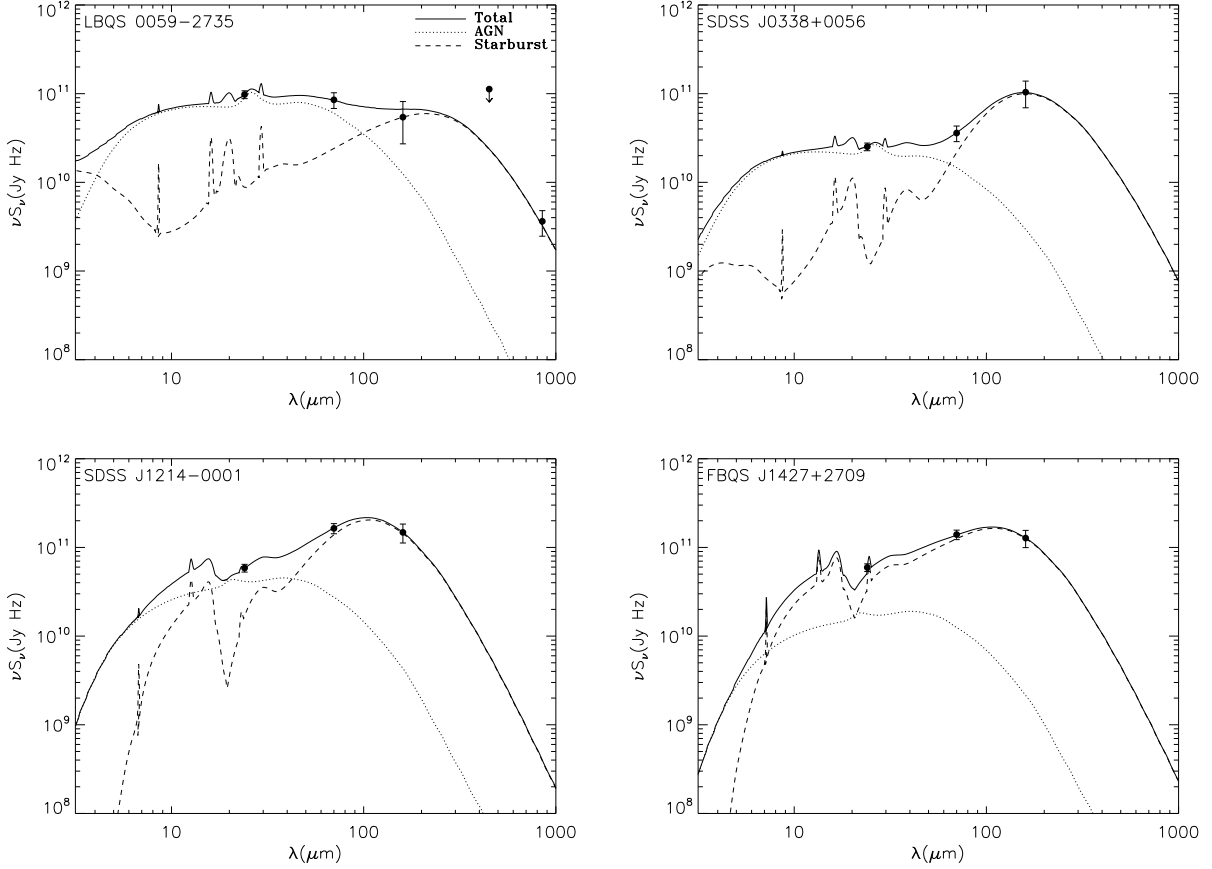


Fig. 1.— Best-fit observed-frame SEDs for the four objects with detections in all three MIPS bands. The best fits have a starburst and AGN component in all four cases, though an AGN contribution to the IR emission is required only in LBQS 0059-2735. The fits do not provide any constraints on the contribution from a starburst or an AGN in the near/mid-IR, or on spectral features (e.g. PAH luminosities). The fits do however illustrate that a starburst is required to explain the emission at longer wavelengths, while remaining consistent with the $24\mu\text{m}$ and $70\mu\text{m}$ fluxes. Error bars are 1σ while upper limits are 3σ .

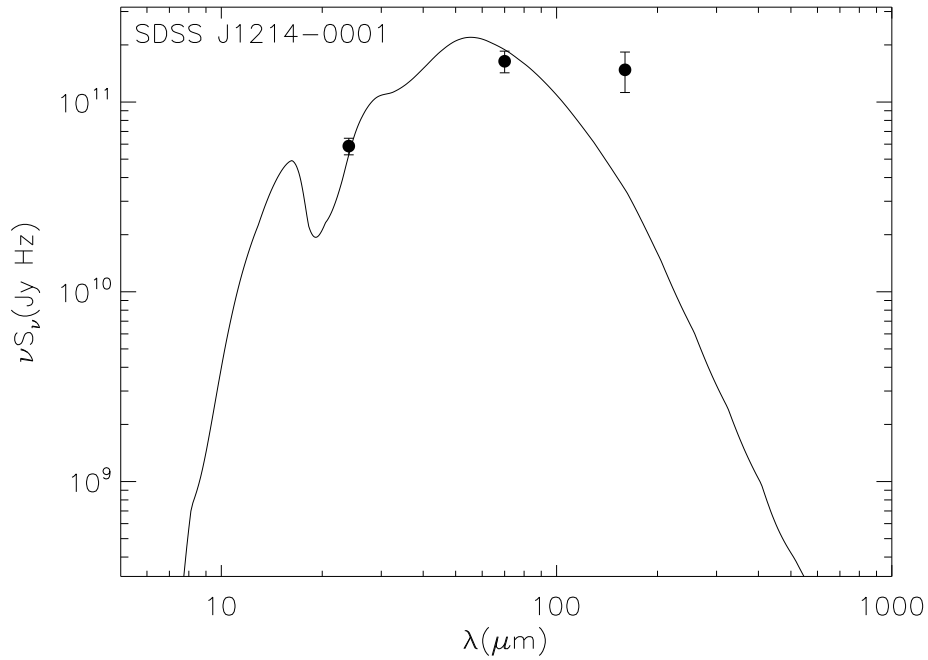


Fig. 2.— An example of an observed-frame pure AGN fit to one of the four objects in our sample with detections at longer wavelengths, in this case the best possible pure AGN fit to SDSS J1214-0001. Here the AGN model differs from that in the lower left panel of Figure 1; the torus is viewed nearly edge-on, leading to a very high inferred obscuration and a strong absorption feature at rest-frame $9.7\mu\text{m}$. Even with such a model however, the fit misses the $160\mu\text{m}$ point by a wide margin.